Proceedings of the Institute of Acoustics

IDENTIFICATION OF POTENTIAL AIRBORNE NOISE PROBLEMS AT THE DESIGN STAGE IN THE LAYOUT OF COMPARTMENTS IN A SUBMARINE

S J Clampton (1), E Rider (1)

(1) Noise & Vibration Engineering Department (NAVED), Vickers Shipbuilding & Engineering Limited (VSEL).

ABSTRACT

Airborne noise is an important factor in setting the environmental conditions under which personnel have to work and rest within the confines of a submarine. Control of airborne noise is thus essential if the safe and efficient running of the submarine is to be maintained. The aim of this paper is to show the importance of identifying potential airborne noise problems at the design stage in the layout of compartments in a submarine.

To show some of the problems that can be encountered when airborne noise is not given full consideration at the design stage, the paper uses as an example the case of a fan plenum initially sited purely on space considerations next to a bunkspace. Once it was found that the fan emitted excessive airborne noise levels, which would cause severe problems in the bunkspace, only then was a full noise assessment made and a series of noise reduction measures proposed. These are discussed in the paper together with the final solution which involved costly reworking of steelwork in the plenum and the installation of a different type of fan. The paper concludes with steps that should have been taken, with hindsight, to reduce the airborne noise problem before compartment layout plans were finalised.

1. INTRODUCTION

1.1 Airborne noise generated within a submarine gives rise to three main problems: a) enhancement of the vessel's overboard radiated noise signature - if this occurs then the risk of the submarine being detected by enemy sonar will increase and with it, exposure to attack; b) increasing sonar self-noise - compromising the submarine's own sonars with extraneous noise will impede both the detection of enemy vessels and safe navigation; c) environmental hazards - these can cause detrimental effects on the ship's crew, ranging from permanent hearing damage to fatigue and communication difficulties. Of the three potential problems due to airborne noise outlined above, the environmental hazard is addressed in this paper.

1.2 Airborne noise in a submarine compartment is generated from three predominant types of noise source: a) machines in that compartment; b) connected systems, such as ventilation and piping, passing through that compartment; c) machines in adjacent compartments.

1.3 In order to minimise hearing risk to the crew, Recommended Noise Levels (RNLs) for each compartment are set by the Institute of Naval Medicine, to take potential airborne noise problems and the type of compartment into account. Generally speaking, those compartments expected to be noisy such as machinery spaces and fan plenums are allocated higher RNLs than say offices, messes and bunkspaces where quieter environments are necessary.

1.4 In order to emphasise the potential problems that can be encountered when airborne noise is not given due consideration at the design stage, the example discussed here illustrates what can happen when airborne noise problems are only addressed during the latter stages of the boat build. Ideally, if it is known from previous experience on submarines, or by theoretical predictions that airborne noise levels in a compartment are liable to exceed the RNL for that space, then various acoustic treatments are considered.

1.5 Examples of palliative measures used are: a) the application of insulation to the compartment boundary surfaces, b) the placing of acoustic hoods or enclosures over machines, and/or c) the fitting of silencers to fans. Such features are more easily accommodated if included at the submarine design stage rather than at the build stage, since by then it may not be possible to fit them, mainly due to lack of space.

1.6 The example considered in this paper concerns the proposed siting of a fan plenum adjacent to a bunkspace, and the high airborne noise levels that would have resulted in that space if the fan in the plenum had been operated.

2. THE PROBLEM

2.1 Space in a submarine is very limited and ideal acoustic considerations even at the design stage are not always practical to install. In the past, for geographical convenience, potentially noisy compartments have been sited next to quiet areas. However, with adequate knowledge and experience of such problems concerning similar machinery noise sources, solutions have been put into effect to remedy this.

2.2 The positioning of a fan plenum adjacent to a bunkspace has occurred on several classes of submarine. Prior to the submarine class discussed here, acoustic insulation fitted on all of the internal boundaries of the fan plenum, except for the deck, reduced the noise transmitted to the bunkspace to an acceptable level.

2.3 However, for the submarine class discussed here, RNLs had become more stringent, the layout of the spaces was slightly different (Figures 1a & 1b) and heavier duty fans were operationally required. Even so, since the acoustic insulation on previous classes was considered more than adequate, it was decided to reduce the insulation fit for the class studied here. Thus at the design stage it was only considered necessary, rather less from an analytical standpoint than an economic one, to attach permanent Constrained Layer Damping (CLD) panels only to the common plenum/bunkspace bulkheads in order to reduce noise transmitted through them (Figure 2).

2.4 This proposal was accepted and construction of the plenum, bunkspace and other compartments was commenced. It was only near the completion of the build that the heavier duty fan to be installed in the plenum underwent its routine pre-installation noise and vibration test. During this test it was found that the airborne noise emitted from this fan exceeded its acceptance levels. It was at this stage that theoretical predictions were carried out to see what effect this would have in compartments near to the fan plenum if the fan was installed. Since the bunkspace had the lowest RNL, the effort was concentrated on this area and it was calculated that a level far in excess of the RNL could be expected in this compartment when the fan was in operation.

2.5 The rather obvious reason why this fan was noisier than previous designs was that it was much larger, outputting more power and hence noise. However, difficulties had occurred in procuring such a fan since specifications dictated that it was required to operate at several different duty states and, in order to meet all the requirements of air flow, pressure, etc., of these duty states, noise aspects of the fan design had been compromised. Meanwhile all construction work in the area of the submarine where the fan was to be installed was halted until a solution was found.

2.6 Calculations showed that, due to the particular combination of plating thickness of enclosure boundaries, the dominant noise transmission paths were not as expected and were via the deck and deckhead rather than through the common bulkheads between the two compartments (Figure 3). It was also found that the CLD panels on the common bulkheads, although giving good attenuation above 2 kHz, had negligible effect on the dominant fan levels below this value.

3. THE SOLUTION

3.1 Various options were put forward to reduce the transmission of noise from the plenum to the bunkspace, not all however, were practical to fit. Altering the thickness of the plenum bulkhead, deck and deckhead plating was dismissed as was the re-arrangement of the plenum/bunkspace layout, both due to the expense and time that would be involved at such a late stage in the boat build. Also, because of the lack of space, inlet and outlet fan silencers could not be fitted. Since the majority of the noise is emitted from the inlet and outlet of the fan, without the silencers, cladding of the fan casing would have yielded little benefit.

3.2 As a first attempt, therefore, to reduce noise levels in the bunkspace and still retaining the original fan, the effect of applying acoustic insulation to the boundary surfaces in the fan plenum was calculated using an acoustic modelling software package developed by NAVED. For the particular plenum in question, two types of insulant would be required. It was possible to fit the discharge chamber with a standard mineral wool insulant widely used throughout the boat, thereby obviating the need and therefore expense of special materials but the suction chamber of the plenum however, required insulation with a waterproof facing because of the possibility of an ingress of sea water in that area.

3.3 Experience based on previous calculations, showed that a thickness of 50 mm of both insulants was required because of their good noise absorption properties around 1 kHz where the highest source levels occurred. By application of the relevant materials to the suction and discharge chambers, except for the suction deck where sea water could accumulate, it was calculated that noise levels in the plenum and bunkspace would be reduced by 4 dBA. It was predicted that the deck and deckhead would remain the dominant transmission paths as before.

3.4 Calculations were then made to determine the effect of replacing the mineral wool in the discharge and suction chambers with one containing a lead core, also used elsewhere within the boat. The lead cored version reduced the contained noise in the plenum by an amount equal to the previous mineral wool insulant, however, it was considerably more effective in reducing the transmitted noise through the plenum boundaries to the bunkspace. An additional reduction, in this space, of 7 dBA could be achieved but would still place the bunkspace outside its RNL.

3.5 Unfortunately it was subsequently discovered that a waterproof faced version of this insulant for application to the suction side of the plenum was not available. Calculations showed that, by using the mineral wool insulant with waterproof facing in the suction chamber and the lead cored insulant in the discharge side of the plenum, a reduction of only 2 dBA could be achieved. An additional few dBA reduction could be achieved by applying insulation to the bunkspace boundaries, but this proposal was rejected due to the difficulties in moulding the insulant around the various domestic fitments in this space.

3.6 At this stage it was evident that it would be highly unlikely that the RNL in the bunkspace could be achieved with the particular fan in question. Attempts to find an alternative, quieter fan which achieved the same duty specifications but which was economically viable failed. Further investigations showed, however, that if some of the ventilation trunks associated with the plenum were re-routed to other fans and various duct valve arrangements were incorporated to effect this operation, then some of the load on the original fan could be shared out among the others already fitted in the boat. This meant that a smaller fan than the original could be used to achieve the remaining duty state requirements with a resulting reduction in source noise.

3.7 This indeed was the partial solution adopted, and a fan which could operate at the duties required for the remaining functions of the original fan was sought. Fortunately a suitable type of fan currently used to fulfil other purposes in submarines and held as a stores item was available. Calculations showed that if this new, smaller fan was installed in the fan plenum in place of the original, a reduction of about 30 dBA could be achieved with no additional acoustic treatments fitted. Also the increased space would allow an inlet and outlet silencer to be fitted to the fan which would result in a further 10 dBA reduction in the bunkspace.

3.8 The frequency spectrum of the smaller fan was such that, by applying the previously investigated fit of mineral wool insulant with waterproof facing on the bulkheads and deckhead of the suction chamber, and the lead cored version on all surfaces in the discharge side of the plenum, a further reduction of 13 dBA in the bunkspace would be achieved. With this insulation fit, calculations showed the dominant noise transmission paths to be via the deckhead and deck of the suction side of the plenum.

3.9 Further acoustic treatment in the form of additional CLD panels were attached between the mineral wool insulation and the bulkheads and deckhead of the suction side of the plenum (Figure 4) and on the underside of its deck. The CLD fit with the new fan had greater effective attenuation than with the original fan because of the high frequency content of its noise spectrum, and an additional 6 dBA reduction in the noise level in the bunkspace was achieved, placing the overall noise level within the RNL. Table 1 summarises the predicted attenuation achieved with the various acoustic treatments in achieving this solution.

3.10 This final insulation fit was accepted, a new fan obtained and work was commenced on the re-routing of the relevant ventilation ducts and manufacture of the new fan support structure in the plenum. The new fan has yet to be tested in situ onboard, however, from past experience in the use of the analysis methods used in the prediction it is fully expected that the RNL will be met.

4. CONCLUSIONS

4.1 As illustrated by the preceding solution, by accommodating the required acoustic analysis at the design of the compartment layout, much time, effort and cost would have been saved later in the boat build stage. With hindsight, the problem outlined here could have been minimised, or even avoided had the larger size of fan been fully recognised as causing potential noise problems and its associated noise levels predicted accordingly. Also acoustic treatments should be selected on the basis of matching their maximum acoustic performance wherever possible to the frequency range within which the noise problem exists.

IDENTIFICATION OF POTENTIAL AIRBORNE NOISE PROBLEMS

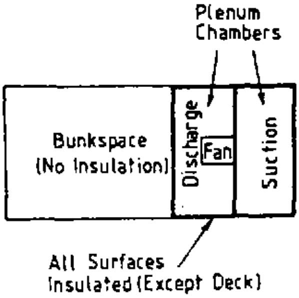

Fig.1a. Simplified Plan View of Plenum & Bunk Space on Previous Class.

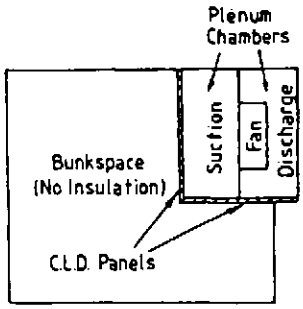

Fig.1b. Simplified Plan View of Plenum & Bunk Space on Class Under Study.

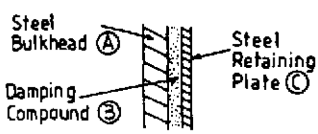

Fig.2. Constrained Layer Damping Panel.

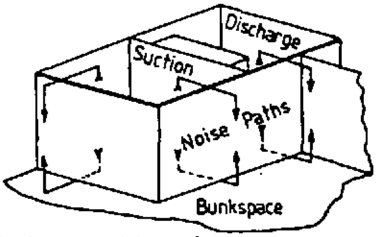

Fig.3. Dominant Noise Paths Between Compartments.

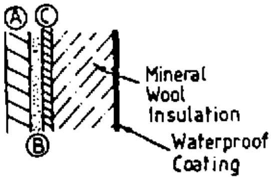

Fig.4. C.L.D. Panel with Added Insulant.

IDENTIFICATION OF POTENTIAL AIRBORNE NOISE PROBLEMS

TABLE 1 PREDICTED ATTENUATION ACHIEVED WITH ACOUSTIC TREATMENTS

ACOUSTIC FIT	TOTAL REDUCTION FROM ORIGINAL FIT (dBA)	RNL
Original fan with CLD panels on common plenum/bunkspace bulkheads (original fit).	-	above
Original fit with mineral wool insulation on all discharge chamber surfaces and waterproof faced mineral wool insulation on all suction chamber surfaces except the deck.	4	above
Original fit with lead cored mineral wool insulation on all discharge chamber surfaces and waterproof faced lead cored mineral wool insulation on all suction chamber surfaces except the deck.	11	above
Original fit with lead cored mineral wool insulation on all discharge chamber surfaces and waterproof faced mineral wool insulation on all suction chamber surfaces except the deck.	6	above
New fan with CLD panels on common plenum/bunkspace bulkheads.	29	above
New fan with inlet and outlet silencers, and CLD panels on common plenum/bunkspace bulkheads.	36	above
New fan with inlet and outlet silencers, CLD panels on common plenum/bunkspace bulkheads, lead cored mineral wool insulation on all discharge chamber surfaces, and waterproof faced mineral wool insulation on all suction chamber surfaces except the deck.	52	above
New fan with inlet and outlet silencers, CLD panels on all suction chamber surfaces (underneath in the case of the deck) and on the common discharge chamber/bunkspace bulkhead, lead cored mineral wool insulation on all discharge chamber surfaces, and waterproof faced mineral wool insulation on all suction chamber surfaces except the deck.	58	below

APPLICATION OF A RECIPROCITY TECHNIQUE FOR THE DETERMINATION OF THE CONTRIBUTIONS OF VARIOUS REGIONS OF A VIBRATING BODY TO THE SOUND PRESSURE AT A RECEIVER POINT.

J M Mason & F J Fahy

University of Southampton, Highfield, Southampton, England

1. INTRODUCTION

Interior noise of frequencies greater than about 400 Hz in private cars is often determined largely by airborne radiation from the vibrating surfaces of the engine and ancillary systems. It is difficult to separate airborne noise from structure-borne noise (through engine mounts, suspensions, etc.) without making expensive and time-consuming alterations to the structural connections. The principle of acoustic reciprocity offers an alternative and convenient means of separating these two components, while at the same time providing information on the relative contributions of various regions of the vibrating engine surface to the noise received at the ears of the passengers or driver.

Presented in this report are results that demonstrate that total received airborne noise may be separated into contributions from contiguous sub-areas of a baffled, point-excited vibrating panel. The use of phase-independent power measurements is considered for the case when no simple reference to the excitation phase is available.

2. LIST OF SYMBOLS

f	frequency (Hz)
G	Green function (m - theory, $kgm^{-4}s^{-1}$ - exper.)
G_{ij}	cross spectrum
H	transfer function
n	unit vector (m)
p	acoustic pressure (Nm^{-2})
Q	volume velocity (m^3s^{-1})
r	position vector (m)
S	body surface (m^2)
v	velocity (ms^{-1})
V	voltage (V)
δS	panel surface elemental area
ρ	density (kg/m^3)
ω	circular frequency ($=2\pi f$)

Subscripts

e	at observation point
g	at vibration generator terminals
i,j	integer variables
n	normal
p	at panel surface

Note the convention $X = \tilde{X}e^{j\omega t}$ is used for complex quantities.

3. THEORY

The sound field radiated by a vibrating solid body into a surrounding fluid is determined solely by the shape of the body and the distribution of vibrational acceleration normal to its surface. This fact is expressed mathematically by the Helmholtz-Kirchhoff integral equation

$$p(r) = \int_S \left[\frac{\partial p(r_s)}{\partial n}\right] G(r,r_s)\, dS \tag{1}$$

where r is the observer point, r_s is a surface point, $\partial p/\partial n$ is the gradient of acoustic pressure normal to the body surface (proportional to the normal acceleration) and G is the Green function which satisfies the condition of zero normal gradient on the body surface. For bodies of complex shape, G takes complicated forms which are not easily calculable, even by modern numerical methods. However, G may be measured simply by placing a small, omni-directional source at a selected receiver point, and measuring the transfer function between acoustic pressure on the surface of the passive body and the volume velocity of the (calibrated) source (Fig.1). Equation (1) may be rewritten as

$$p(r) = -i\omega\rho_0 \sum_i (v_i\, \Delta S)\, G_i(r,r_s), \tag{2}$$

since $\frac{\partial p}{\partial n} = -i\omega\rho_0 v$. Noting that $v_i\,\Delta S = Q_i$, surface volume velocity, reciprocity gives

$$\frac{p(r)}{Q_i} = -i\omega\rho_0\, G_i(r,r_s) = \frac{p_i}{Q(r)}.$$

Equation 2 may be rearranged to the form

$$p(r) = \sum_i (v_i\,\Delta S)\frac{p_i}{Q(r)}. \tag{3}$$

In equation (3) it is seen that the method consists of approximating the surface integral of equation (1) by a summation over a set of discrete points on the body surface. The acceleration of the running engine is measured at the same set of points as the transfer functions and combined with the latter to predict the sound pressure at the receiver point. The result is valid provided that (i) the whole system behaves linearly, (ii) a sufficient density of measurement points is selected. The technique accounts for <u>all paths</u> between the engine surface and the receiver point, irrespective of whether they involve structural vibration or not. Clearly, it is possible to assess the relative contributions of the various regions on the engine to the received sound pressure, and to predict the effect of suppressing them.

4. EXPERIMENTATION

The technique was validated by tests in a normal laboratory on a system consisting of a five-sided, heavy box to which was clamped a 6.25 mm thick panel on the open side: this thickness is thought to be reasonably representative of typical, average block casting thicknesses. The panel had surface dimensions 48cm x 48cm, when clamped into a 5.33 cm wide frame along all edges (see fig. 2). The panel was excited by a vibration generator (a magnet and coil assembly inside the box) using band-limited random noise and the drive voltage V_g was used as a reference to the excitation. Normal velocity v_p, was measured on a grid of 81 points over the panel using an accelerometer. Sound pressure p_p was measured at the surface of the panel at the same locations as v_p. An observation point was chosen to provide a direct line of sight to the panel. A 2.54cm thick, large chipboard panel was inserted between the observation point and box to remove the direct path. An existing, calibrated omni-directional source Q_e was used in the experiments, placed so as to be acoustically coincident with the microphone p_e at the observation point.

Each experiment divided into two halves. Firstly, with panel excited by the shaker, the transfer function $\tilde{p}_e/\tilde{V}_g$ was measured, i.e. the 'referenced' pressure at the observation point. In addition, the transfer functions $(\tilde{v}_p/\tilde{V}_g)_i$ were acquired for each of the i=1 to 81 sub-areas of the panel. Secondly, with the volume velocity source at the observation point providing the excitation, the transfer functions $(\tilde{p}_p/\tilde{Q}_e)_i$ were acquired, again for each of sub-areas of the panel. From equation 3 for discrete measurements we have:

$$\frac{\tilde{p}_e}{\tilde{V}_g} = \sum_{i=1}^{81} \left[\frac{\tilde{p}_p}{\tilde{Q}_e}\right]_i \left[\frac{\tilde{Q}_p}{\tilde{V}_g}\right]_i , \qquad (4)$$

where $\tilde{Q}_p = \tilde{v}_p.\delta S$. Two experimental configurations are considered here. These are for

(i) the direct path present between the observation point and the simple panel,
(ii) the direct path blocked between the observation point and a non-uniform panel.

The non-uniform panel was identical to the uniform panel except for an aluminium slab of dimensions 16cm x 16 cm x 1.25 cm, glued to the underside (see fig. 3). Along with the direct path there existed secondary paths via nearby walls, ceiling, equipment and cupboards. These dominated when the direct path was obstructed.

5. RESULTS

The result shown in figure 4, for the first case, gives the comparison between the direct measurement and the prediction (comprising 162 transfer functions and calibration). Although discrepancies arise in a few narrow bands the agreement is generally good. Figure 5 shows the relative phase between the two, which should (of course) be zero at all frequencies. Large phase inaccuracies are only seen to occur at points of low response.

Figure 6 show the result for case (ii), and a similar degree of agreement is found. It is noted that the response is reduced, in most frequency bands, with the introduction of the screen and is improved, at lower frequencies, by the addition of the inhomogeneity.

5.1 Influence of point density.

The radiation of sound from the panel is related to transverse bending waves excited in the panel, and a coherent near field local to the point of excitation. Adequate point density is determined by the need to represent the smallest acoustic wavelength to be radiated by the panel. [Since the panel critical frequency is around 2000Hz, over most of range of analysis (400-2000Hz) the radiation efficiency will be low]. At 2000Hz, the wavelength of sound in air at 20°C is 0.17m, so the chosen measurement grid used to generate the results shown (figs 4-6) is clearly adequate to comply with the minimum requirement of half-wavelength sampling. If the data from the previous results is reprocessed using only 9 points (a 3 x 3 array, each sub-area δS had dimensions 16cm x 16cm) then it is reasonable to expect severe discrepancy between direct and predicted levels, at least down to 1050Hz, below which adequate sampling is still predicted. It was found that a favourable comparison exists below 700Hz, but above this the consequence of undersampling is apparent. Generally the phase information in the prediction is no longer correct.

5.2 Diagnostics.

Once it has been verified that the multi-pathed prediction is satisfactorily close to the direct measurement, then it is possible to perform some diagnostics tests on the data. It is simple, in the first instance, to see the effect of the removal of any one path on the result of the remaining summation, i.e. if one path is acoustically treated (and assumed to be removed, without altering anything else about the system) how will this effect the pressure level at the observer point? Figure 7 shows such an analysis for case (i) (simple panel, direct field present), in terms of changes in third octave bands. The reduction (or enhancement) of sound pressure at the observer point is indicated in grey-scale for each sub-area of the panel as it is removed from the summation (equation (2), note cell A is the best to treat, B is the worst). It is possible that the best areas indicated for treatment correpond to anti-nodal regions of panel modes, or, in the case of 397Hz third octave band, that a coherent near-field to the excitation point is seen. The improvement due to the omission of any one cell is small, due to the large number of cells and the uniformity of the panel.

It is not possible to verify these changes experimentally since they are within the limits of experimentally accuracy (= 2 to 3dB repeating the same complete experiment). A more clear cut result might be expected in the more complex geometry and non-uniformity of an actual engine block. It must be remembered that the results shown correspond to the effect of the removal of the contributions of individual squares. Before acoustically treating a larger area of adjacent black squares the analysis should be repeated for the omission of all the removed cells together.

5.3 Absence of a 'Reference'.

The drive voltage to the shaker coil, in the experiment described above, provides a very good reference since it is 'flat' in frequency terms and is completely correlated with the excitation. In the case of engine block, where the noise generated is due to a number of processes, no simple reference to the excitation exists. An alternative arbitrary reference could be adopted, such as the pressure at a point near to the engine, or a measurement scheme involving the acquisition of cross-spectra could be used. Under this scheme the transfer functions $H_i = (\tilde{p}_p/\tilde{Q}_e)_i$ are acquired as before and structure surface vibration is represented by cross spectra measurements $G_{ij} = \tilde{v}_i\tilde{v}_j^*$, then

$$\tilde{p}\tilde{p}^* = |\tilde{p}|^2 = \sum_i \sum_j H_i H_j^* G_{ij} \tag{5}$$

It would be understandably tempting to dispose of the need for a reference to vibration and make simple estimates, viz

$$|\tilde{p}|^2 = \sum_i H_i H_i^* G_{ii}\,, \tag{6}$$

where $G_{ii} = \tilde{v}_i\tilde{v}_i^* = |\tilde{v}|^2$, the vibration autospectra. For the case of a panel vibrating at frequencies not much below its critical frequency, this should lead to an error in the predicted sound level since the omitted cross-terms are still expected to make a definite contribution. In addition, it is reasonable at lower frequencies that a coherent near-field region around the point of excitation on the structure may dominate the observed sound pressure. In this case an underestimate may be obtained, since the enhancement due to adjacent cells vibrating in phase is neglected. The analysis suggested in equation 6 was performed on the data obtained in the above experiments, i.e.

$$\left|\frac{\tilde{p}_e}{\tilde{V}_g}\right| = \left[\sum_i \left|\frac{\tilde{p}_p}{\tilde{Q}_e}\right|_i^2 \left|\frac{\tilde{Q}_p}{\tilde{V}_g}\right|_i^2\right]^{1/2}, \tag{7}$$

and compared with the prediction obtained by the linear analysis (equation 4). The result for test (i) is shown, in 1/3 octave bands, in figure 8. Generally, a significant underestimate is produced by the approximation of equation 7.

If the sound pressure level at the observation point is determined simply by a forced panel response local to the point of excitation, then it is possible to obtain an accurate prediction using only contributions from the local sub-areas, neglecting the rest of the panel. The summation in equation 4 has been repeated for 28 'local' squares (cf figure 7) and the vibrational 'near-field' prediction is compared with the direct and whole-panel prediction results in figure 9, once again in third octave bands. At low frequencies the observed pressure is dominated by the near-field since the 'near-field' prediction is seen to be roughly equal to the direct measurement. At higher frequencies, the near field progressively shrinks and other parts of the panel contribute more efficiently as the critical frequency is approached. The near-field prediction tends towards an underestimate of 6dB since only a third of the panel data has been used.

6. CONCLUSIONS

It has been demonstrated that the sound pressure at an observation point may be obtained by summing the contributions of contiguous sub-areas from a baffled, point-excited vibrating panel, with reasonable accuracy. It follows that the relative contributions of the sub-areas of the panel to the sound pressure at the observation point may be determined. In principle, insight into the efficient application of acoustic treatment to the radiating surface may be obtained from the acquired data. Along with the condition of system linearity it is also requirement of this technique that adequate discretisation of the radiating surface is implemented. The use of simple power estimates that neglect phase information has been shown to be flawed.

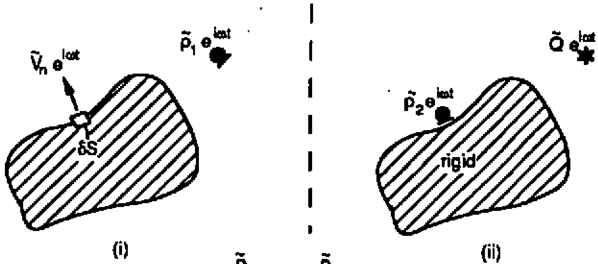

$$\frac{\tilde{p}_1}{\tilde{v}_n \delta S} = \frac{\tilde{p}_2}{\tilde{Q}} = -i\omega\rho\tilde{G}$$

Figure 1. Reciprocal measurement of the Green function

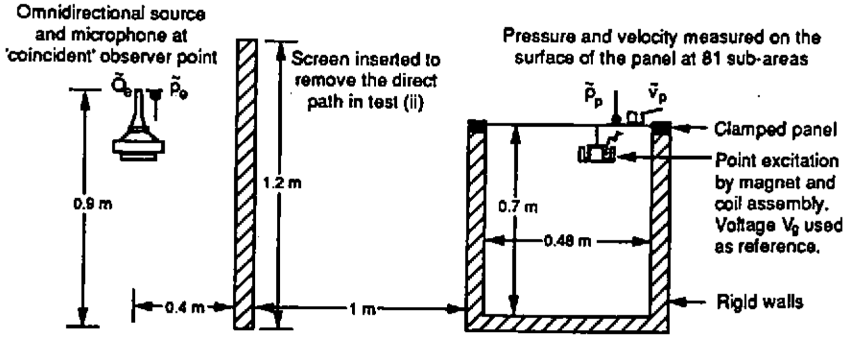

Figure 2. The test rig.

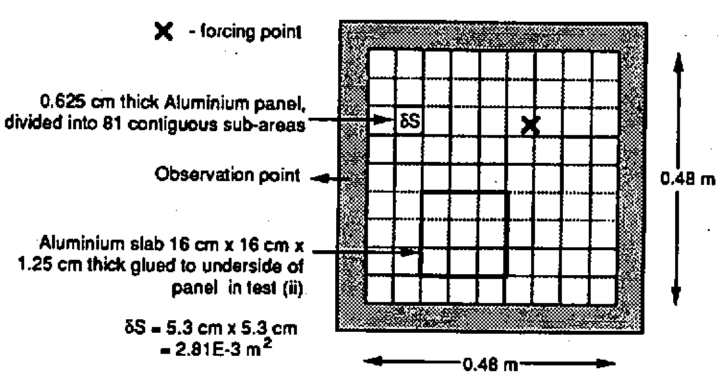

Figure 3. Description of panels used in the tests

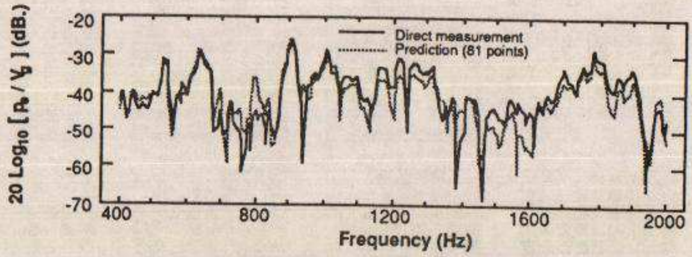

Figure 4. Comparison of direct and predicted pressure magnitude at the observation point for test (i) (simple panel, direct path present).

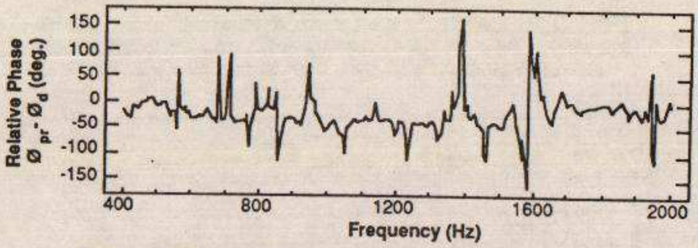

Figure 5. Relative phase between direct and predicted pressure at the observation point for test (i) (simple panel, direct path present).

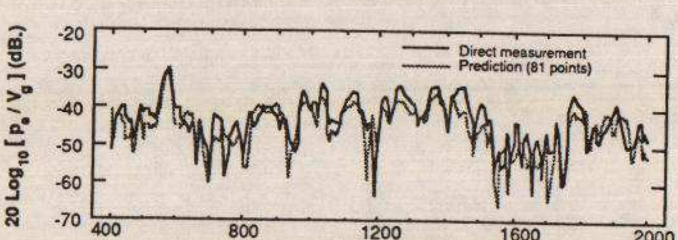

Figure 6. Comparison of direct and predicted pressure magnitude at the observation point for test (ii) (non-uniform panel, direct path blocked).

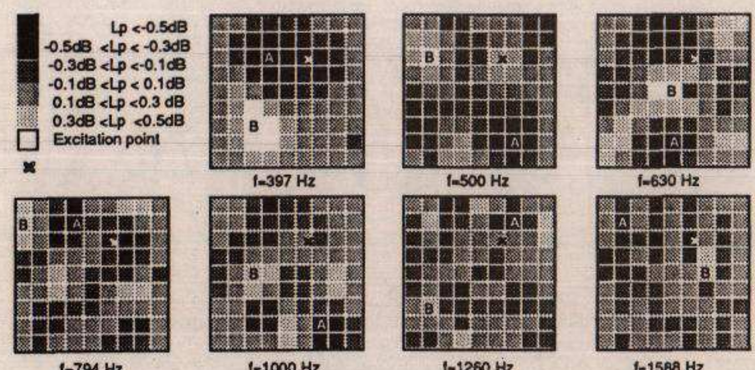

Figure 7. Schematic of the effect of removing the contribution of individual sub-areas of the panel to the observation point pressure, for test (i) (simple panel, direct path present). Note: black squares are the best to treat.

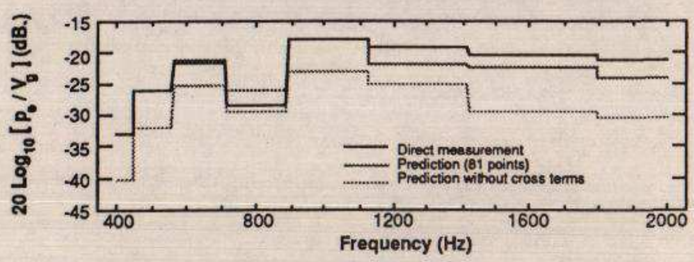

Figure 8. Comparison of direct, predicted and 'simple estimate excluding cross-terms' pressure magnitude in 1/3 octave bands at the observation point for test (i) (simple panel, direct path present).

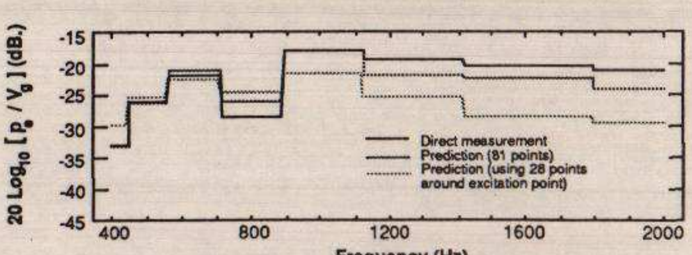

Figure 9. Comparison of direct, predicted and 'excitation near field estimate' pressure magnitude in 1/3 octave bands at the observation point for test (i) (simple panel, direct path present).